IER3 supports KRAS[G12D]-dependent pancreatic cancer development by sustaining ERK1/2 phosphorylation

Maria Noé Garcia,[1] Daniel Grasso,[1] Maria Belen Lopez-Millan,[1] Tewfik Hamidi,[1] Celine Loncle,[1] Richard Tomasini,[1] Gwen Lomberk,[2] Françoise Porteu,[3] Raul Urrutia,[2] and Juan L. Iovanna[1]

[1]Centre de Recherche en Cancérologie de Marseille (CRCM), INSERM U1068, CNRS UMR 7258, Aix-Marseille Université and Institut Paoli-Calmettes, Parc Scientifique et Technologique de Luminy, Marseille, France. [2]Laboratory of Epigenetics and Chromatin Dynamics, Gastroenterology Research Unit, Departments of Biochemistry and Molecular Biology, Biophysics, and Medicine, Mayo Clinic, Rochester, Minnesota, USA. [3]INSERM U1009, Gustave Roussy Cancer Campus, Université Paris XI, Villejuif, France.

Activating mutations in the *KRAS* oncogene are prevalent in pancreatic ductal adenocarcinoma (PDAC). We previously demonstrated that pancreatic intraepithelial neoplasia (PanIN) formation, which precedes malignant transformation, associates with the expression of immediate early response 3 (*Ier3*) as part of a prooncogenic transcriptional pathway. Here, we evaluated the role of IER3 in PanIN formation and PDAC development. In human pancreatic cancer cells, IER3 expression efficiently sustained ERK1/2 phosphorylation by inhibiting phosphatase PP2A activity. Moreover, IER3 enhanced *Kras*[G12D]-dependent oncogenesis in the pancreas, as both PanIN and PDAC development were delayed in IER3-deficient *Kras*[G12D] mice. IER3 expression was discrete in healthy acinar cells, becoming highly prominent in peritumoral acini, and particularly high in acinar ductal metaplasia (ADM) and PanIN lesions, where IER3 colocalized with phosphorylated ERK1/2. However, IER3 was absent in undifferentiated PDAC, which suggests that the IER3-dependent pathway is an early event in pancreatic tumorigenesis. IER3 expression was induced by both mild and severe pancreatitis, which promoted PanIN formation and progression to PDAC in *Kras*[G12D] mice. In IER3-deficient mice, pancreatitis abolished *Kras*[G12D]-induced proliferation, which suggests that pancreatitis enhances the oncogenic effect of KRAS through induction of IER3 expression. Together, our data indicate that IER3 supports KRAS[G12D]-associated oncogenesis in the pancreas by sustaining ERK1/2 phosphorylation via phosphatase PP2A inhibition.

Introduction

Pancreatic ductal adenocarcinoma (PDAC) is likely to stem from a process known as acinar-to-ductal metaplasia, which involves either transdifferentiation of adult acinar cells or aberrant differentiation of their progenitors into ductal-like cells. These cells can subsequently progress into malignant adenocarcinoma through a series of histopathological lesions known as pancreatic intraepithelial neoplasias (PanINs) (1). Activating mutations in the gene encoding the GTPase KRAS are nearly universal in human PDAC (2), and targeting of mutated *KRAS* to mouse pancreatic progenitors recapitulates the human PanIN-to-PDAC progression sequence (3). Early pancreatic lesions, including low-grade PanINs, already carry an activating *KRAS* mutation (4), which indicates that mutation in this oncogene is one of the earliest events in the pathophysiology of PDAC. High-grade lesions develop upon accumulation of further mutational events, mainly involving inactivation of other tumor suppressors such as *INK4A* (also known as *CDKN2A*, *P16*, or *ARF*), *TP53*, *SMAD4*, or *BRCA2* (5). Several genetic and epigenetic factors (regulating senescence, autophagy, cell cycle, and apoptosis) may positively or negatively modulate the transforming activity of mutant *KRAS* in pancreatic cells, thereby modulating PanIN development. Among these factors, we recently described a novel intracellular pathway essential for KRAS transforming

activity in the pancreas controlled by the pancreatitis-activated protein NUPR1 (also known as p8 or COM1), which involved RELB, but not RELA (6). We demonstrated that genetic deletion of *Nupr1* in mice inhibits *Kras*-dependent PanIN development in a *Relb*-dependent manner. We also found that in this genetic context, *Relb* activation is dependent on *Nupr1* expression. Consequently, pancreatic-specific deletion of *Relb* in a *Kras*[G12D] background resulted in delayed PanIN development. In addition, we found that disruption of this novel NUPR1-RELB transcriptional pathway affects the expression of genes encoding proteins that can serve as effectors of their function, such as immediate early response 3 (*IER3*) (6). Thus, efficient PanIN formation is dependent on *Nupr1* and *Relb* expression, with likely involvement of *Ier3*. However, the defined role of *IER3* in PanIN development and its molecular mechanism remain to be established.

IER3 (also known as IEX-1, p22/PRG1, Dif-2, or gly96) belongs to the immediate early response gene family (7, 8). *IER3* is a stress-inducible gene exerting divergent effects on cellular responses in stressed cells. IER3 displays complex and sometimes divergent roles in cell cycle, differentiation, and survival depending on the cell type and stimulus under study (7–11). The multiple cellular actions exerted by IER3 involve antagonism of various signaling pathways, in particular those regulated by ERKs. ERK activation involves a cascade of phosphorylation events, initiated by stimulation of RAS and ultimately leading to MEK1/2-mediated dual phosphorylation of ERK1/2 at neighboring Ser/Thr and Tyr residues in the activation loop (12). The ERK pathway is implicated in

diverse cellular processes, including proliferation, differentiation, and survival. This variety of biological responses is determined by the cell-specific combination of downstream substrates and differences in the magnitude and kinetics of ERK signaling (13, 14). The length of time that ERKs are active depends on the nature of the stimuli, the cooperation of several pathways downstream of RAS, the localization of the kinases, or the presence of scaffold proteins (12). It has been shown that IER3 prolongs ERK phosphorylation and ERK activation, thereby triggering phosphorylation of ERK substrates (15). This effect of IER3 involves direct interaction with the regulatory PP2A subunit B56. By bridging ERK to B56, IER3 contributes to ERK-dependent phosphorylation of B56, with subsequent dissociation from the catalytic PP2A subunit and, consequently, potentiation of ERK signaling (16). This reduced B56-regulated PP2A activity causes sustained ERK1/2 activation with concomitant phosphorylation of several target proteins (17).

Previous studies in human cancers have revealed differential expression for IER3 not only in tumor versus normal tissue, but also in the same tumor type of different disease stages. Positive IER3 expression is associated with good prognosis in ovarian cancer, where IER3 functions as a proapoptotic factor to restrict tumor growth (18, 19). On the contrary, a high level of IER3 expression appears to link poor survival of patients with multiple myeloma (20–25), Sézary syndrome (26–28), and breast cancer (29), in part due to a prosurvival effect of IER3 on cancer cells. In myelodysplastic syndromes, IER3 expression increases gradually with disease development toward acute myeloid leukemia (23, 24). Finally, IER3 appears to play distinct roles in different subsets or stages of colon cancer (30–32) as well as pancreatic cancer (6, 33, 34). Thus, the definitive roles of IER3 in the initiation, promotion, and/or progression of these gastrointestinal malignancies remain to be defined. Here, we sought to elucidate whether IER3 plays a role in $Kras$ oncogene–driven PanIN-to-PDAC formation, using well-characterized engineered mouse models for pancreatic cancer. We found that deletion of $Ier3$ delayed PanIN development in $Pdx1$-$Cre;LSL$-$Kras^{G12D}$ (referred to herein as $Kras^{G12D}$) animals. In addition, deletion of $Ier3$ significantly reduced PDAC incidence and consequently extended the survival of compound $Kras^{G12D};Ink4a^{fl/fl}$ animals. Moreover, we showed that IER3 expression was induced by tumor-promoting stimuli such as pancreatitis, which, in the presence of oncogenic $Kras$, acts as a well-known tumor-promoting mechanism. However, pancreatitis in $Ier3^{-/-}$ mice abolished the growth-promoting role of this oncogene. Mechanistically, we found that these effects of IER3 on pancreatic cancer growth occurred primarily by a role of this protein in enhancing ERK1/2 phosphorylation through an inhibitory effect on PP2A phosphatase activity. These observations extend our understanding of molecular mechanisms underlying pancreatic carcinogenesis and identify IER3 as a potential target for therapies aimed to control the oncogenic potential of $Kras$.

Results

IER3 is expressed in acinar ductal metaplasia (ADM), PanINs, and peritumoral acini in both murine and human pancreatic cancers. To better dissect the role of IER3 in PDAC development in vivo, we used 2 complementary mouse models. The $Kras^{G12D}$ mouse model is the tool of choice for studying initial, well-differentiated pretumoral lesions, since these mice reproducibly develop metaplasia

and PanINs at about 12 weeks of age (6). The $Kras^{G12D};Ink4a^{fl/fl}$ model serves specifically to simulate poorly differentiated PDAC; these animals develop aggressive tumors at 8 weeks of age (35). Immunofluorescent (IF) analysis of normal pancreas tissue showed no detectable IER3 signal in acinar cells, regardless of the status of activated $Kras^{G12D}$ (Figure 1A). In contrast, PanINs, independent of grade, displayed high levels of IER3 in $Kras^{G12D}$ pancreas at 20 weeks of age (Figure 1A). In 8-week-old $Kras^{G12D};Ink4a^{fl/fl}$ mice, IER3 expression was detected in well-differentiated glandular structures within PDAC tumors and principally in the peritumoral acini and low-grade PanINs. Interestingly, IER3 staining was faint or absent in poorly differentiated tumor cells (Figure 1B), although it was highly expressed in ADM lesions. These observations were also confirmed in pancreas lesions from another well-known animal model, the $Mist1;Kras^{G12D};Trp53^{+/-}$ transgenic mouse (36), which develops a more differentiated type of tumor that shares several characteristics with human PDAC (Supplemental Figure 1; supplemental material available online with this article; doi:10.1172/JCI76037DS1). Moreover, similar to our observations in $Kras^{G12D};Ink4a^{fl/fl}$ mice, we found undetectable levels of IER3 in normal human pancreatic tissue, whereas morphologically normal acini located at the periphery of human PDAC showed substantial IER3 staining (Figure 1C). Similarly, IER3 levels decreased in preneoplastic lesions in the progression from well-differentiated to poorly differentiated, being strong in low-grade PanINs but barely detectable or undetectable in more advanced grades (Figure 1C). We also examined the expression of $IER3$ in 2 groups of patients who, upon immunohistochemical (IHC) analysis, presented features of well-to-moderately differentiated PDAC. This experiment confirmed that $IER3$ expression was higher in well-to-moderately differentiated human adenocarcinoma (well-to-moderately differentiated, 3.93 ± 2.05 AU, $n = 10$; poorly differentiated, 0.41 ± 0.20 AU, $n = 12$; $P < 0.05$; Figure 1D). In summary, the results obtained by both IF and IHC staining of mouse and human tissues revealed upregulation of IER3 within discrete acinar cells that became more prominent in larger acinar clusters, especially those located near PDAC, and particularly high in ADM and low-grade PanINs. Thus, high levels of IER3 appear to be necessary during the early events of pancreatic carcinogenesis, likely helping to establish the process of initiation.

IER3 depletion delays Kras^{G12D}-driven PanIN and PDAC development. To determine whether pretumoral lesions and PDAC development require the presence of IER3, we generated 2 novel mouse lines by crossing $Kras^{G12D}$ and $Kras^{G12D};Ink4a^{fl/fl}$ mice with $Ier3^{-/-}$ mice (37). At least 12 inbred crosses were made for each new transgenic mouse line before evaluation in order to assure a homogeneous genetic background. All mice were viable, fertile, and showed no obvious abnormality. As illustrated in Figure 2A, control $Kras^{G12D};Ier3^{+/+}$ littermates exhibited ADM as well as low- and high-grade PanINs at 14 weeks (ADM, 7 ± 1.3 lesions per field of view; PanIN 1a, 2.4 ± 0.5; PanIN 1b, 3.6 ± 0.4; PanIN 2, 1.2 ± 0.4; PanIN 3, 0.4 ± 0.2; $n = 5$). In addition, 100% of those mice contained at least 1 lesion in the pancreas. $Kras^{G12D};Ier3^{+/-}$ mice also harbored ADM and low-grade PanINs, albeit in reduced numbers (ADM, 2.2 ± 1.2 lesions per field of view; PanIN 1a, 0.8 ± 0.4; PanIN 1b, 0.4 ± 0.2; PanIN 2, 0.2 ± 0.2; PanIN 3, 0; $n = 5$) and 60% of these mice presented at least 1 lesion in pancreas.
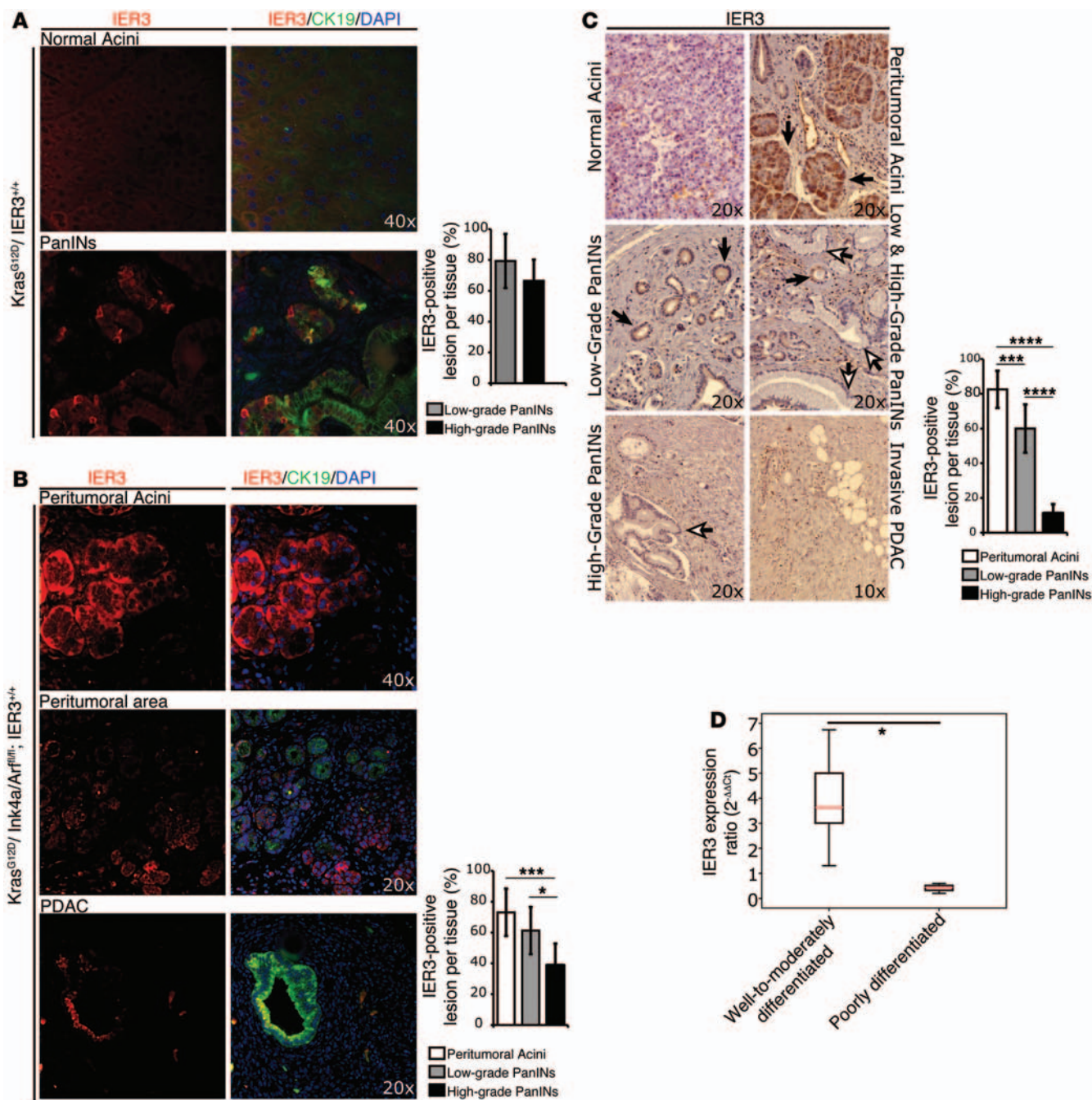
Figure 1. IER3 expression in pancreas. (**A** and **B**) IF for IER3 (red) and CK19 (green) in paraffin-embedded tissue sections obtained from 20-week-old *Kras^G12D* mice and 8-week-old *Kras^G12D;Ink4a^fl/fl* mice. Percentage of IER3-positive lesions per tissue is also shown (*n* = 9 [**A**]; 8 [**B**]). (**C**) IHC analysis of IER3 on human pancreatic samples. Peritumoral acini and low-grade PanINs (black arrows) were positive for IER3, whereas high-grade PanINs (white arrows) showed almost undetectable IER3 staining. Percentage of IER3-positive lesions per tissue is also shown (*n* = 14 tumor samples). (**D**) Real-time quantitative PCR analysis for *IER3* expression in human adenocarcinoma samples from well-to-moderately differentiated (*n* = 10) and poorly differentiated (*n* = 12) tissues. Error bars denote ± SEM; *P* values were calculated by $2^{-\Delta\Delta Ct}$ method. *$P < 0.05$, ***$P < 0.001$, ****$P < 0.00001$. Original magnification, ×40 (**A** and **B**, top); ×20 (**B**, middle and bottom, and **C**).

Careful analysis of *Kras^G12D;Ier3^-/-* animals revealed the presence of even fewer numbers of ADM and PanIN 1b lesions (2 of 5 mice; ADM, 1 ± 0.5 lesions per field of view; PanIN 1b, 0.6 ± 0.4), with no PanIN 2 or PanIN 3 lesions observed. These differences were statistically significant among different genotypes and lesion types in 14-week-old mice (*P* < 0.0001). Similar results, although with

more pronounced differences between genotypes, were obtained at 25 and 40 weeks of age (*P* < 0.0001 for both; Figure 2A). Figure 2B shows representative PanINs developing at 40 weeks in the different genotypes. *Kras^G12D;Ier3^+/+* mice had a large number of high-grade PanINs with abundant positive periodic acid–Schiff (PAS) staining. Moreover, IF for both amylase and cytokeratin
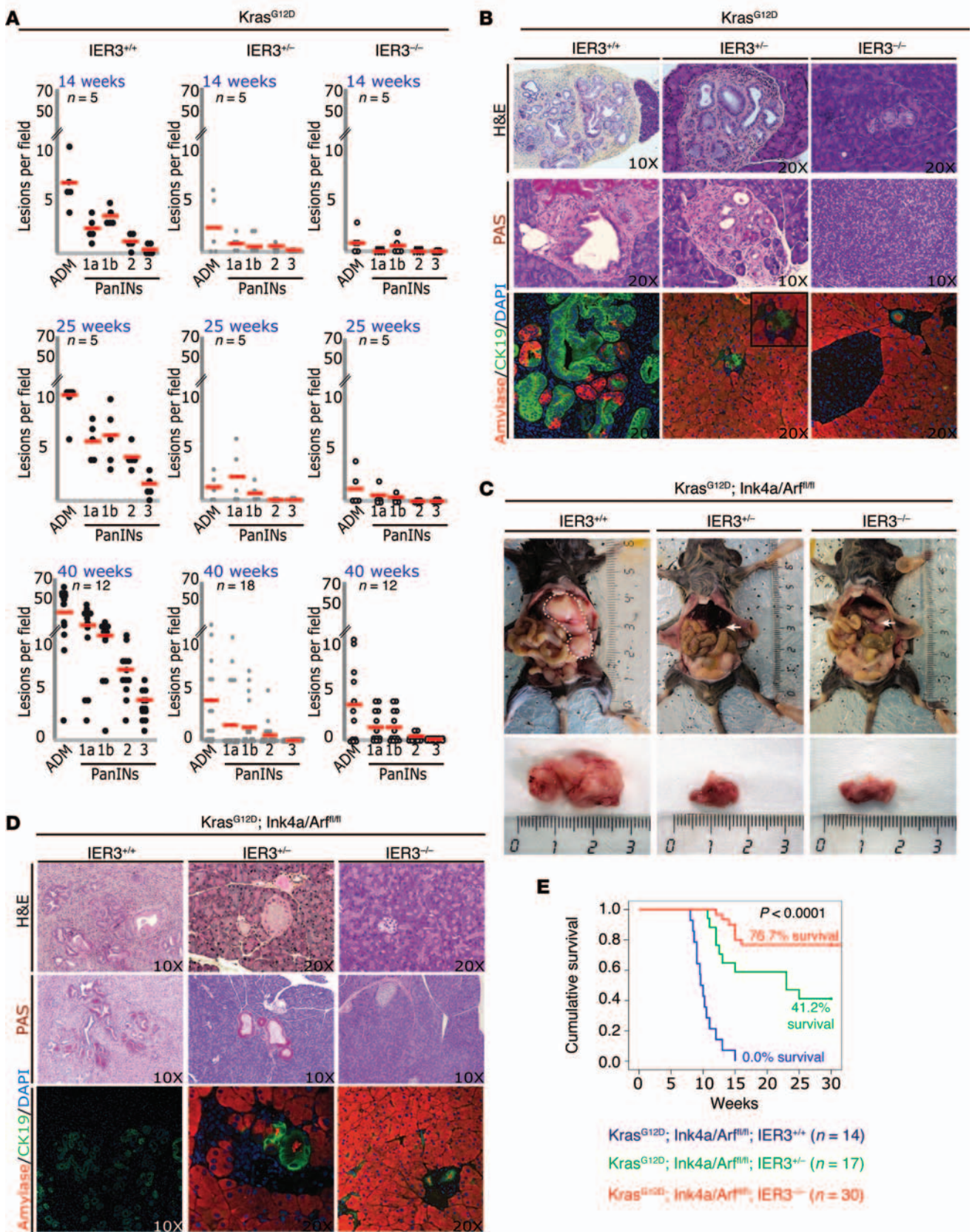
Figure 2. Induction of PanINs and PDAC by Kras^{G12D} oncogene requires IER3 expression. (A) Number of ADM and PanIN lesions per ×20 tissue field in *Kras^{G12D};Ier3$^{+/+}$*, *Kras^{G12D};Ier3$^{+/-}$*, and *Kras^{G12D};Ier3$^{-/-}$* mice at 14, 25, and 40 weeks of age. Horizontal bars denote means. Differences among genotypes and lesion types were significant at all ages (*P* < 0.0001). **(B)** Pancreas tissue paraffin sections from *Kras^{G12D};Ier3$^{+/+}$*, *Kras^{G12D};Ier3$^{+/-}$*, and *Kras^{G12D};Ier3$^{-/-}$* mice at 40 weeks of age. Shown are H&E staining, mucin content of PanINs highlighted by PAS staining, and IF for amylase (red) and CK19 (green). **(C–E)** Analysis of *Kras^{G12D};Ink4a$^{fl/fl}$;Ier3$^{+/+}$*, *Kras^{G12D};Ink4a$^{fl/fl}$;Ier3$^{+/-}$*, and *Kras^{G12D};Ink4a$^{fl/fl}$;Ier3$^{-/-}$* mice. **(C)** Macroscopic images showing pancreas (arrows) of 8-week-old littermates. Dashed outline denotes PDAC. **(D)** Mouse pancreas paraffin sections at 8 weeks of age. Shown are H&E staining, mucin content of PanIN PAS staining, and IF for amylase (red) and CK19 (green). **(E)** Kaplan-Meier analysis of cumulative survival. Differences were significant among genotypes (*P* < 0.0001). Original magnification, ×10 and ×20 (**B** and **D**, as indicated); ×30 (**B**, inset).

19 (CK19) revealed replacement of the acinar for the ductal cell marker. In contrast, lesions of any type were not frequently found in *Kras^{G12D};Ier3$^{-/-}$* pancreases, which also stained negative with the PAS technique (Figure 2B). Thus, these genetic modeling experiments led us to conclude that IER3 expression is indeed necessary for *Kras^{G12D}*-mediated initiation in the exocrine pancreas.

Subsequently, we investigated the role of IER3 during more advanced steps of PDAC carcinogenesis by crossing *Ier3$^{-/-}$* mice with *Kras^{G12D};Ink4a$^{fl/fl}$* mice, which carry inactivation of the tumor suppressor *Ink4a* (whose loss exerts tumor promotion of *Kras^{G12D}*-positive preneoplastic cells into cancer). At 8 weeks of age, *Kras^{G12D};Ink4a$^{fl/fl}$;Ier3$^{+/+}$* mice developed PDAC with 100% penetrance (*n* = 8), as demonstrated by PAS-positive malignant cells with complete loss of amylase immunostaining and mild staining for CK19 (Figure 2, C and D). In contrast, 8-week-old *Kras^{G12D};Ink4a$^{fl/fl}$; Ier3$^{+/-}$* mice retained substantial areas of normal pancreas and did not develop PDAC (*n* = 8). In fact, only 37.5% of these animals developed ADM and low-grade PanINs (<5% of lesions per pancreas), with few CK19-positive ductal lesions containing PAS-positive cells compared with *Kras^{G12D};Ink4a$^{fl/fl}$;Ier3$^{+/+}$* littermates. Finally, 8-week-old *Kras^{G12D};Ink4a$^{fl/fl}$;Ier3$^{-/-}$* mice showed large areas of normal tissue, composed of amylase-positive, PAS-negative cells, which never gave rise to PDAC (*n* = 8). Thus, deletion of *Ier3* impaired development of frank pancreatic cancer even upon deletion of *Ink4a*, a potent stimulus for tumor promotion in this organ. We also evaluated the long-term contribution of IER3 to *Kras^{G12D}*-driven PDAC development by performing Kaplan-Meier survival analyses (Figure 2E). *Kras^{G12D};Ink4a$^{fl/fl}$;Ier3$^{+/+}$* mice had 0.0% survival (100% mortality; *n* = 14) at 30 weeks of evaluation, with mean survival of 10.27 ± 0.52 weeks. Meanwhile, *Kras^{G12D};Ink4a$^{fl/fl}$;Ier3$^{+/-}$* mice had 41.2% survival, with 7 of 17 mice reaching 30 weeks of age without tumor or any other sign of disease. Interestingly, although *Kras^{G12D};Ink4a$^{fl/fl}$;Ier3$^{+/-}$* animals exhibited mean survival of 21.6 ± 1.97 weeks (Figure 2E), the Kaplan-Meier curve evidenced 2 different behaviors: one showing mean survival of 12.3 ± 0.51 weeks, and the other with mean survival of 23.6 ± 1.15 weeks (Figure 2E). More surprisingly, *Kras^{G12D};Ink4a$^{fl/fl}$;Ier3$^{-/-}$* mice had 76.7% survival, with only 7 of 30 (23.3%) developing PDAC, with mean survival of 27.86 ± 1.37 weeks. Notably, only 7 *Kras^{G12D};Ink4a$^{fl/fl}$;Ier3$^{-/-}$* mice developed PDAC (mean survival, 14.3 ± 1.38 weeks), a delay of 4 weeks compared with *Kras^{G12D};Ink4a$^{fl/fl}$;Ier3$^{+/+}$* mice. Comparative statistical analyses of survival curves among the 3 genotypes showed significant differences (*P* < 0.0001). These results collectively demonstrated that IER3 is an important contributor to ADM, PanIN, and PDAC development by oncogenic *Kras*, either alone or in combination with *Ink4a* deletion.

IER3 plays a direct effect on pancreatic oncogenic transformation. Since IER3 is a well-established regulator of the immune system (8), we sought to rule out the possibility that IER3-mediated impairment of ADM and PanIN formation was not in fact through an indirect effect. We first used the innovative method of Bar-Sagi and colleagues (38, 39), which relies on isolation of pancreatic ductal epithelial cells (PDECs) from *Kras^{G12D};Ier3$^{+/+}$* and *Kras^{G12D};Ier3$^{-/-}$* animals and their transduction with Cre-encoding adenovirus (referred to herein as Ad-Cre). In this setting, we observed increased BrdU incorporation in the Cre-transduced PDECs from *Kras^{G12D};Ier3$^{+/+}$* pancreas compared with cells transduced with null control adenovirus (Ad-null; Figure 3A). No statistically significant increase was detected in *Kras^{G12D};Ier3$^{-/-}$* PDECs treated in the same manner (Figure 3A). We also evaluated the ability of acini isolated from *Kras^{G12D};Ier3$^{+/+}$* or *Kras^{G12D};Ier3$^{-/-}$* pancreas to form ADM in vitro after *Kras^{G12D}* activation by Ad-Cre. Importantly, morphological examination of the acini from *Kras^{G12D};Ier3$^{-/-}$* mice showed a 25.0% ± 2.98% incidence of ADM events after Ad-Cre transduction (Figure 3B). In contrast, Cre-mediated *Kras^{G12D}* activation produced ADM-like structures on only 10.5% ± 1.29% of *Kras^{G12D};Ier3$^{-/-}$* acini (Figure 3B). Together, these results demonstrated that IER3 plays an important role in *Kras^{G12D}*-dependent ADM development in vitro in the absence of any external stimulus, including the immune system.

IER3-dependent ERK phosphorylation contributes to pancreatic tumorigenesis. IER3 has been previously shown to undergo phosphorylation by ERK1/2 and can also potentiate the activation of these kinases in response to several growth factors in different nonpancreatic cell types (15). Thus, to investigate whether IER3 is involved in the regulation of ERK1/2 activity in pancreatic cancer cells, we evaluated the effect of its depletion on these signaling proteins. We knocked down IER3 expression in human pancreatic cancer cells using siRNA and subsequently monitored ERK1/2 phosphorylation (p-ERK1/2). After 48 hours of IER3 siRNA treatment of MiaPaCa2 cells, IER3 protein levels decreased approximately 95%, with a concomitant 45% reduction in p-ERK1/2 (Supplemental Figure 2, A and B). Comparable results were observed in Panc1 cells, with IER3 reduced 45% and p-ERK1/2 reduced 40% (Supplemental Figure 2, A and B). Control experiments confirmed that activation of the upstream kinase MEK1/2 remained unmodified in both cell lines (Supplemental Figure 2B). These findings were further supported by IF and flow cytometry analyses, which showed a 48% decrease of ERK1/2 activation in response to IER3 depletion (Supplemental Figure 2, C and D). We previously demonstrated that IER3 expression in human pancreatic cell lines decreases upon genetic inactivation of both *NUPR1* and *RELB* (6). We therefore speculated that RELB and NUPR1 could have a role in ERK1/2 activation by affecting IER3 expression. To test this hypothesis, we transfected MiaPaCa2 cells with siRNA against NUPR1 or RELB and measured p-ERK1/2 by Western blot analyses (Supplemental Figure 2G). These
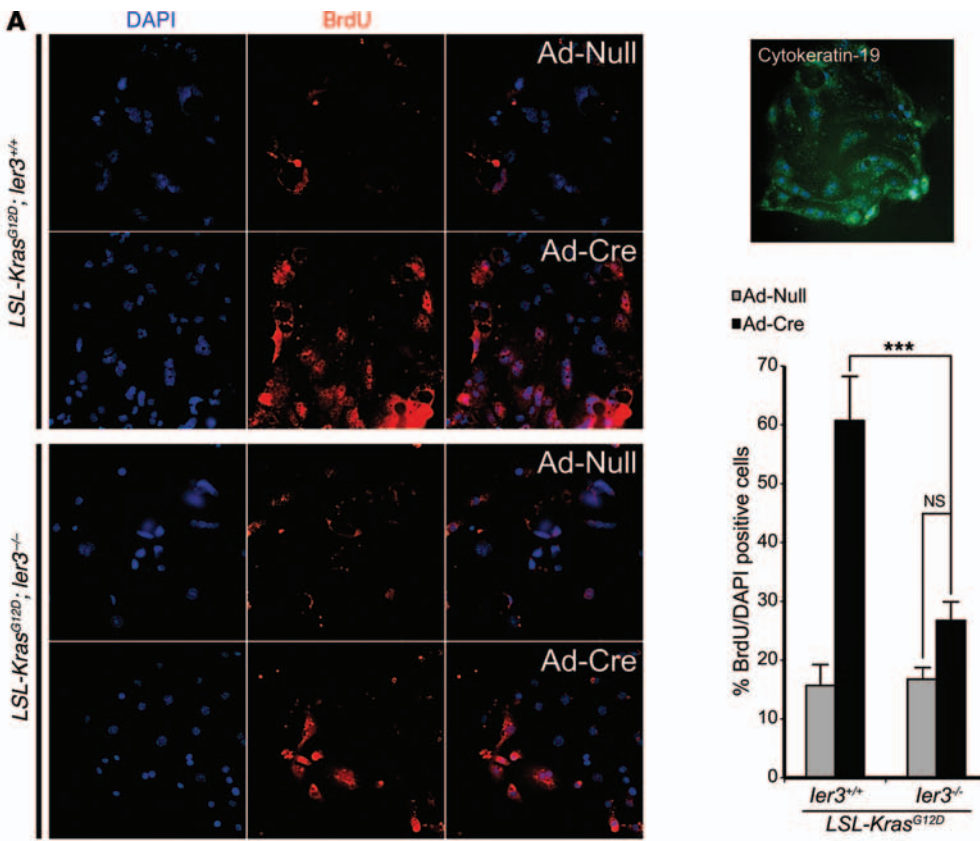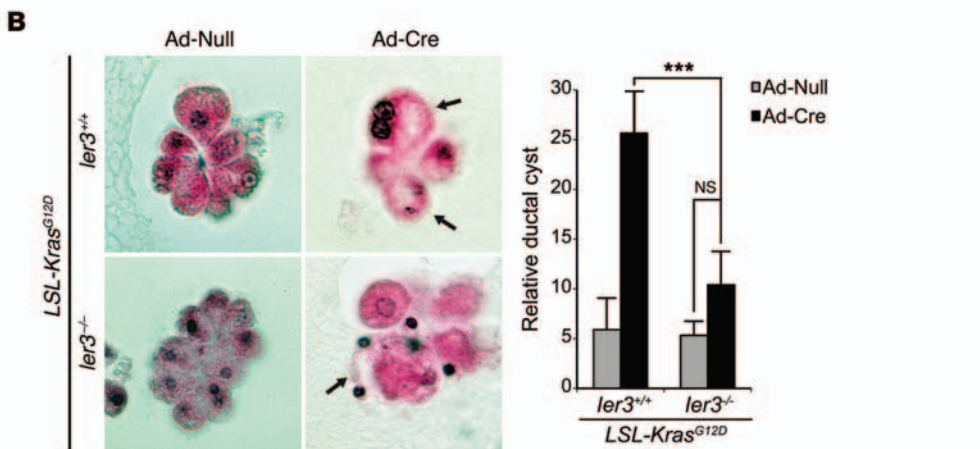
Figure 3. IER3 has a cell-autonomous role in early PanIN development. (**A**) BrdU incorporation IF of PDECs isolated from $Kras^{G12D};Ier3^{+/+}$ and $Kras^{G12D};Ier3^{-/-}$ animals. A substantial growth increase was observed in $Kras^{G12D};Ier3^{+/+}$ PDECs after Ad-Cre–mediated $Kras^{G12D}$ activation. Conversely, in $Kras^{G12D};Ier3^{-/-}$ PDECs, oncogenic $Kras^{G12D}$ activation produced a slight increase in proliferation (albeit not statistically significant) compared with Ad-null–infected control cells. CK19-positive staining confirmed the ductal origin of the cells. (**B**) In vitro ADM in pancreas acini from $Kras^{G12D};Ier3^{+/+}$ and $Kras^{G12D};Ier3^{-/-}$ animals after Ad-Cre or Ad-null infection. The absence of $Ier3$ significantly reduced ADM events after Ad-Cre–mediated $Kras^{G12D}$ activation. ***$P < 0.001$. Original magnification, ×40 (**A**); ×60 (**B**).

experiments showed the siRNA-mediated decreases in NUPR1 and RELB both dramatically decreased p-ERK1/2 (by 49% and 42%, respectively), similar to the results obtained with IER3 knockdown. Moreover, we found that overexpression of IER3 rescued these effects (Supplemental Figure 2G). Similar results were obtained with Panc1 pancreatic cancer cells. Together, these data suggest that activation of ERK1/2 by the NUPR1/RELB pathway is dependent on IER3 expression in pancreatic cancer cells.

Altered p-ERK1/2, but not p-MEK1/2, in the pancreas of $Kras^{G12D};Ier3^{-/-}$ mice. Recent data suggesting that RAS activation must reach a minimum threshold in order to transform the pancreas (40) led us to examine whether IER3 is one of the proteins that modulates the signaling function of this oncogene. We evaluated the activity of its downstream effectors, namely p-MEK1/2

and p-ERK1/2, using IHC. At 14 weeks of age, the pancreases from $Kras^{G12D};Ier3^{-/-}$ mice and $Kras^{G12D};Ier3^{+/+}$ controls exhibited comparable p-MEK1/2 levels (Figure 4A). Nevertheless, active p-ERK1/2 was present in lesions and a few isolated acinar regions of $Kras^{G12D};Ier3^{+/+}$ mice; in contrast, in $Kras^{G12D};Ier3^{-/-}$ pancreas, active p-ERK1/2 was barely detectable (Figure 4A). Quantitatively, we found that the $Ier3^{-/-}$ genotype was associated with reduced p-ERK1/2 levels compared with the control at 14 (0.49 relative units; interquartile range [IQR], 0.35–0.64) and 40 (0.25 relative units; IQR, 0.19–0.33) weeks of age. Similar results were obtained in $Kras^{G12D};Ink4a^{fl/fl};Ier3^{+/+}$ pancreas, which had active p-MEK1/2 at

5 weeks (prior to substantial transformation) and at 8 weeks (PDAC development). Additional experiments using IHC for p-ERK1/2 in 5-week-old $Kras^{G12D};Ink4a^{fl/fl};Ier3^{+/+}$ mice revealed several positive isolated acinar regions (20%–45% of total pancreas; Figure 4B). In stark contrast, 5-week-old $Kras^{G12D};Ink4a^{fl/fl};Ier3^{-/-}$ mice showed no p-ERK1/2 staining. Staining for p-ERK1/2 was also positive at 8 weeks of age in PDAC of $Kras^{G12D};Ink4a^{fl/fl};Ier3^{+/+}$ animals, but negative in $Kras^{G12D};Ink4a^{fl/fl};Ier3^{-/-}$ animals, where it was found to be limited to stromal cells (Figure 4B). The validity of these results was corroborated by Western blot, which showed reduced p-ERK1/2 in $Kras^{G12D};Ink4a^{fl/fl};Ier3^{-/-}$ relative to $Kras^{G12D};Ink4a^{fl/fl};Ier3^{+/+}$ mice at 8 weeks of age (0.33 relative units; IQR, 0.2–0.75; Figure 4B). More importantly, in $Kras^{G12D};Ink4a^{fl/fl};Ier3^{+/+}$ pancreatic tissue, we observed substantial colocalization between IER3 and p-ERK1/2
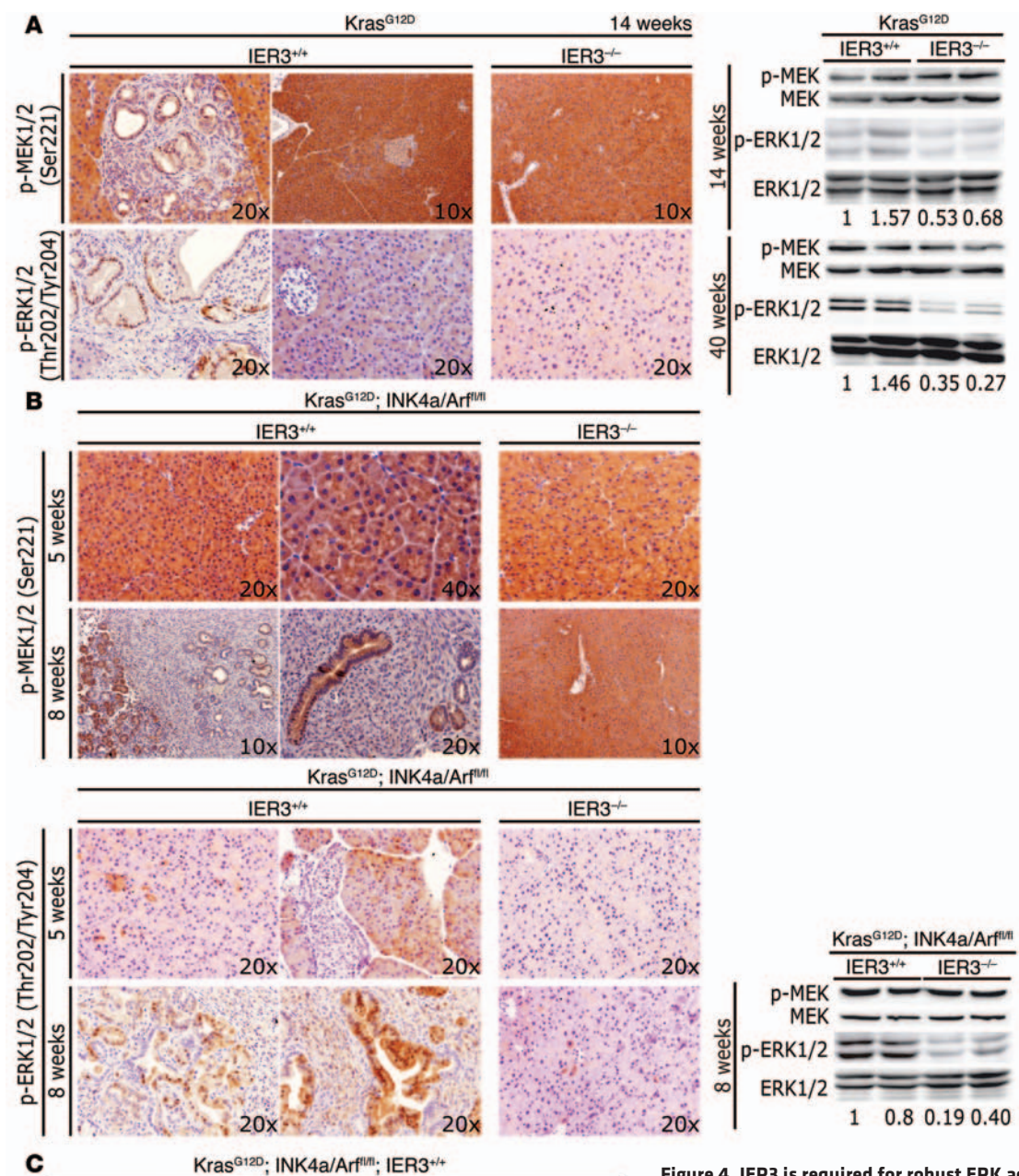
Figure 4. IER3 is required for robust ERK activation.
(**A**) IHC for p-MEK1/2 and p-ERK1/2 at 14 weeks of age and Western blot of p-MEK1/2 and p-ERK1/2 at 14 and 40 weeks from $Kras^{G12D};Ier3^{+/+}$ and $Kras^{G12D};Ier3^{-/-}$ mice in pancreatic lysates. (**B**) IHC for p-MEK1/2 and p-ERK1/2 at 5 and 8 weeks of age and Western blot for p-MEK1/2 and p-ERK1/2 at 8 weeks from $Kras^{G12D};Ink4a^{fl/fl};Ier3^{+/+}$ and $Kras^{G12D};Ink4a^{fl/fl};Ier3^{-/-}$ mice in pancreatic lysates. In **A** and **B**, relative band quantification is shown below blots. (**C**) IF for IER3 (green) and p-ERK1/2 (red) in paraffin sections from a $Kras^{G12D};Ink4a^{fl/fl};Ier3^{+/+}$ mouse. Original magnification, ×10, ×20, and ×40 (**A** and **B**, as indicated); ×40 (**C**).

within PanIN structures (Figure 4C). Together, these results suggest that IER3 is necessary in order to maintain the p-ERK1/2 level required for $Kras^{G12D}$-dependent malignant transformation in vivo.

We studied the tumor growth capacity of the $Kras^{G12D};Ink4a^{fl/fl}$-derived tumor cell lines CKΔI-1 and CKΔI-2 (see Methods), modulating the cells' p-ERK1/2 by expressing HA-IER3, HA-IER3-ΔBD,

HA-IER3-T18A, and ERK2-L73P/S151D (constitutive activated form of ERK) constructs or by knocking down IER3 expression using shRNA. Efficiency of the transfection was controlled by Western blot measurement of p-ERK1/2 levels (Supplemental Figure 3A). Surprisingly, no significant differences in tumor growth were found when the cells were xenografted in nude mice.
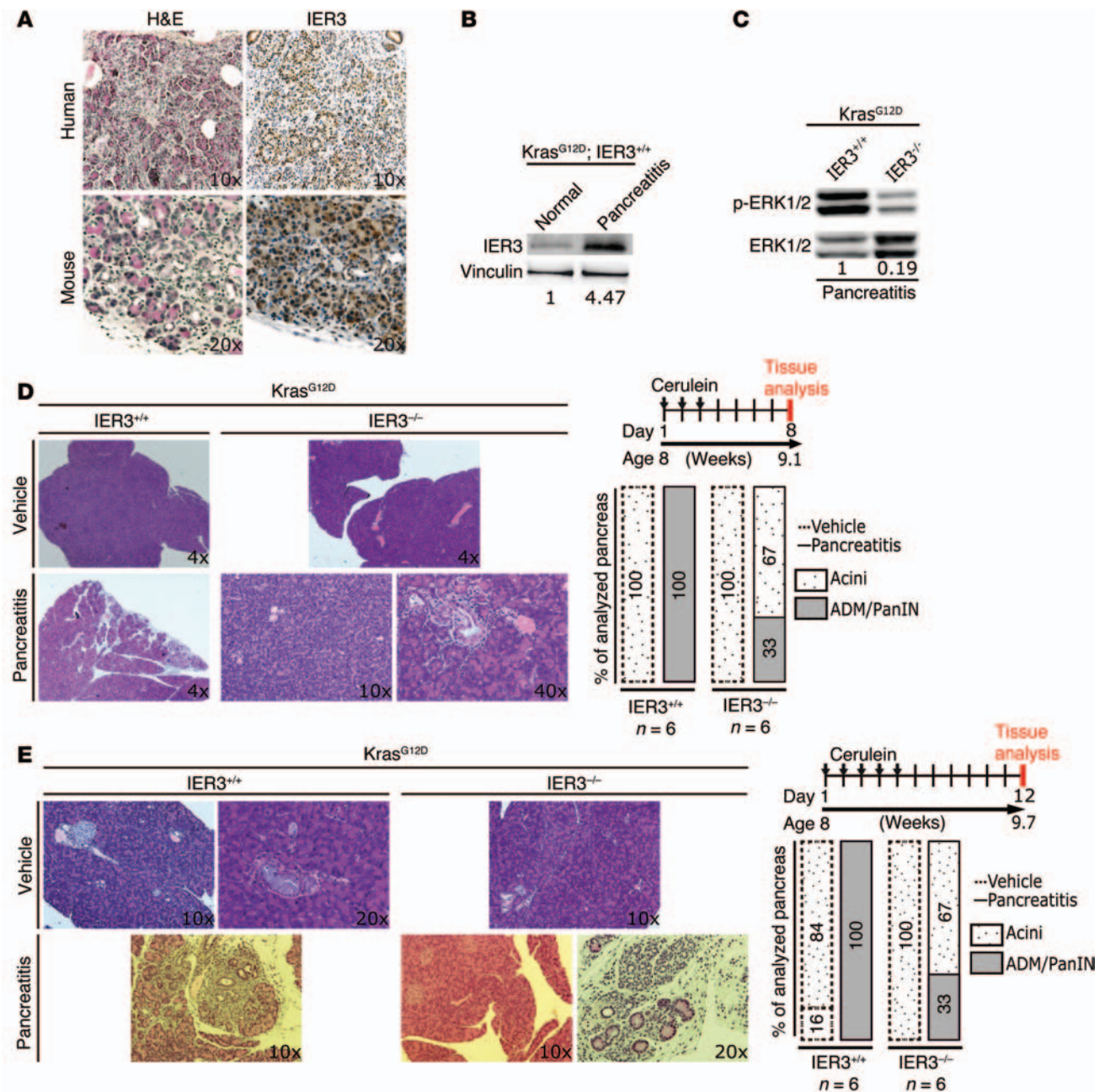
Figure 5. IER3 is overexpressed during pancreatitis. (**A**) H&E and IER3 IHC in peritumoral pancreatitis from human PDAC and experimental pancreatitis from *Kras*^{G12D}*;Ier3*$^{+/+}$ mice. (**B** and **C**) Western blots for IER3 (**B**) and p-ERK1/2 (**C**) in pancreas tissue lysates from *Kras*^{G12D}*;Ier3*$^{+/+}$ and *Kras*^{G12D}*;Ier3*$^{-/-}$ mice upon experimental acute pancreatitis. Relative band quantification is shown below blots. (**D** and **E**) *Kras*^{G12D}*;Ier3*$^{+/+}$ and *Kras*^{G12D}*;Ier3*$^{-/-}$ mice were treated with daily injection of cerulein or vehicle for 3 days followed by 5 days of recovery (**D**), or for 5 days followed by 7 days of recovery (**E**), to assess tissue damage. Shown are treatment schemes, H&E staining of pancreatic tissue sections, and quantified proportions of lesion types in tissue (*n* = 6 per group). Original magnification, ×4, ×10, ×20, and ×40 (**A**, **D**, and **E**, as indicated).

Moreover, both MiaPaCa2 and Panc1 cells (with decreased IER3 expression) grew similarly as xenografts in nude mice (Supplemental Figure 3B). Together, these observations suggested that changes in IER3 expression that effect the intracellular level of p-ERK1/2 have no effect on cell growth of readily cancerous human cell lines. These results support inferences derived from both the expression data in mice and humans and the modeling experiments in *Kras*^{G12D}*;Ink4a*$^{fl/fl}$*;Ier3*$^{-/-}$ mice (Figure 1 and Supple-

mental Figure 3), which together indicate that IER3 plays a role in the early stages of neoplastic transformation.

Pancreatitis-induced tumorigenesis requires IER3 expression. Oncogenic *KRAS* expression, confined to acinar or islet cell compartments, contributes to PDAC formation in the setting of pancreatitis (41, 42). Figure 5A shows the expression of IER3 in inflammation-positive areas within the pancreas of *Kras*^{G12D} mice and in peritumoral-inflamed regions in human PDAC. In these samples,

IER3 expression was elevated in discrete acinar clusters. IER3 expression also increased about 4-fold in *Kras^{G12D}* mice during induction of experimental acute pancreatitis, which was accompanied by p-ERK1/2 activation (Figure 5, B and C). Activation of these MAPKs, however, was markedly lower in *Kras^{G12D};Ier3$^{-/-}$* pancreas (Figure 5C), suggestive of a key role of IER3 in maintaining ERK1/2-dependent signaling. These findings led us to hypothesize that IER3 expression during pancreatitis enhances the transforming properties of oncogenic *Kras^{G12D}*. To test this hypothesis, we treated 8-week-old *Kras^{G12D};Ier3$^{+/+}$* and *Kras^{G12D};Ier3$^{-/-}$* mice with 250 μg/kg of the pancreatitis inducer cerulein. We used 2 cerulein treatment protocols to analyze tissue damage and cancerous lesion induction: the first consisted of daily cerulein injection for 3 days followed by a 5-day recovery period before tissue analysis (Figure 5D); the second, which induced more severe damage, consisted of daily cerulein injection for 5 days followed by a 7-day recovery period (Figure 5E). Interestingly, when applied to *Kras^{G12D};Ier3$^{+/+}$* mice, both pancreatitis induction models caused extensive replacement of the normal pancreatic tissue by fibrosis and inflammation, with the majority of epithelial cells replaced by ADM and PanINs in 100% of cases (*n* = 6 per group; Figure 5, D and E). However, vehicle-treated *Kras^{G12D};Ier3$^{-/-}$* mice had normal pancreases, and pancreatitis-induced *Kras^{G12D};Ier3$^{-/-}$* mice presented only ADM and low-grade PanINs in 33.3% of cases (2 of 6; Figure 5, D and E). Therefore, we concluded that IER3 expression induced by pancreatitis in acinar cells enhances the effect of the *Kras^{G12D}* oncogene. Similar results were obtained using the *Kras^{G12D};Ink4a$^{fl/fl}$* mouse model after inducing tumorigenic development by pancreatitis induction. We treated 5-week-old *Kras^{G12D};Ink4a$^{fl/fl}$;Ier3$^{+/+}$*, *Kras^{G12D};Ink4a$^{fl/fl}$;Ier3$^{+/-}$*, and *Kras^{G12D};Ink4a$^{fl/fl}$;Ier3$^{-/-}$* mice with cerulein daily for 5 days, followed by recovery until 30 weeks of age. If mice did not develop PDAC by this time point, pancreases were removed for examination (Figure 6A). *Kras^{G12D};Ink4a$^{fl/fl}$;Ier3$^{+/+}$* mice subjected to recurrent pancreatitis showed a median survival of 8.44 ± 0.31 weeks with cerulein treatment, compared with 11.40 ± 0.41 weeks with vehicle treatment (*P* < 0.005, log-rank test; Figure 6, B and C). Of the *Kras^{G12D};Ink4a$^{fl/fl}$;Ier3$^{+/-}$* animals, none with pancreatitis survived, compared with 40.0% of the untreated group (*P* < 0.05, log-rank test); in these mice, pancreatitis shortened the median survival time by 5 weeks, from 24.40 ± 2.63 to 19.00 ± 1.14 weeks. Interestingly, 75.0% of *Kras^{G12D};Ink4a$^{fl/fl}$;Ier3$^{-/-}$* mice survived to the expected time, with their pancreases showing normal acini. However, upon induction of pancreatitis, the survival of these animals decreased to 50% (pancreatitis, median survival 20.96 ± 3.2 weeks; vehicle, 26.25 ± 2.30 weeks) and showed ADM and PanINs at 30 weeks. Notably, survival was not significantly different between treatment groups in *Kras^{G12D};Ink4a$^{fl/fl}$;Ier3$^{-/-}$* mice (*P* > 0.05, log-rank test; Figure 6, B and C); this suggests that even though the pancreas was challenged to develop PDAC by cerulein treatment, the lack of *Ier3* enabled animals to withstand the tumorigenic process. However, we still observed significant differences in cumulative survival among the 3 genotypes subjected or not to pancreatitis (*P* < 0.0001, log rank test; Figure 6B). These observations indicate that the requirement for IER3 signaling during PanIN and PDAC development cannot be compensated for by the loss of the tumor suppressors encoded by the *Ink4a* locus (p16/p19), even when tumor promotion is forced by pancreatitis induction.

Discussion

Using genetically engineered mice, we recently demonstrated that *Kras^{G12D}*-dependent PanIN formation required the expression of *Nupr1* (6). Additional experiments suggested that RELB could be one mediator of these effects. This hypothesis was supported by the observation that *Relb*-deficient mice showed a significant delay in PanIN development (6). Consequently, IER3 was selected as a putative mediator of the RELB effect, as a target gene of *Nupr1* and *Relb* (6). These prior studies prompted us to define whether IER3 plays a role in PanIN development. Our present data demonstrated that IER3 expression efficiently sustains p-ERK1/2 and enhances the effects of *Kras^{G12D}* in the pancreas. We also showed that *Nupr1* and *Ier3* were concomitantly induced in the pancreas with pancreatitis, an inflammatory process that promotes PanIN formation and progression to PDAC development in the context of *Kras* oncogenic activation (41, 42). Finally, we demonstrated that NUPR1 and RELB enhance ERK1/2 activation in an IER3-dependent manner, which indicates that these 3 proteins are linked into a single cascade — sequentially, pancreatitis followed by NUPR1, RELB, IER3, and finally p-ERK1/2 — that ultimately supports PanIN development after pancreatitis.

Previous studies using convincing genetic approaches have clearly demonstrated that ERK1/2 activity is critical for *Kras*-dependent tumor development (39). Consequently, all upstream and downstream stimuli affecting ERK1/2 activity could likely regulate both PanIN and PDAC development. In fact, p-ERK1/2 is dependent on the relative balance between kinase and phosphatase activity levels. The PP2A enzyme has long been identified as the major Ser/Thr phosphatase involved in ERK1/2 inactivation (43). PP2A is involved in a broad range of cellular processes (44), and this diversity of functions is conferred by a multiplicity of regulatory subunits. The PP2A holoenzyme is a heterotrimer that consists of a core dimer, composed of a scaffold, and a catalytic subunit that associates with various regulatory subunits. The regulatory subunits have been divided into 3 gene families, named B (also known as PR55), B′ (B56 or PR61), and B″ (PR72), each of which consists of several members (45). The B subunits determine substrate specificity and subcellular localization. B56β or B56γ, but no other B family members, increase PP2A-dependent ERK1/2 dephosphorylation (16). Mechanistically, our experimental evidence supports a model whereby IER3 binds to B56, enhances B56 phosphorylation by ERK1/2, which in turn triggers dissociation from the catalytic subunit and thereby inhibits PP2A, resulting in sustained p-ERK1/2 (16). Hence, through this function, IER3 can serve as a regulator of the oncogenic activity of *Kras^{G12D}*. It is therefore likely that pathological situations that induce IER3 overexpression can associate with sustained ERK1/2 activity and, in this manner, facilitate *Kras^{G12D}* transformation. Here we demonstrated that pancreatitis induces IER3 overexpression and a concomitant increase in active ERK, supporting the hypothesis that pancreatitis enhances the *Kras*-oncogenic role, at least in part, through this mechanism. We provided experimental evidence supporting this hypothesis in vivo by using 2 complementary mouse models of PDAC in which *Ier3* was genetically inactivated. Although the inactivation of *Ier3*
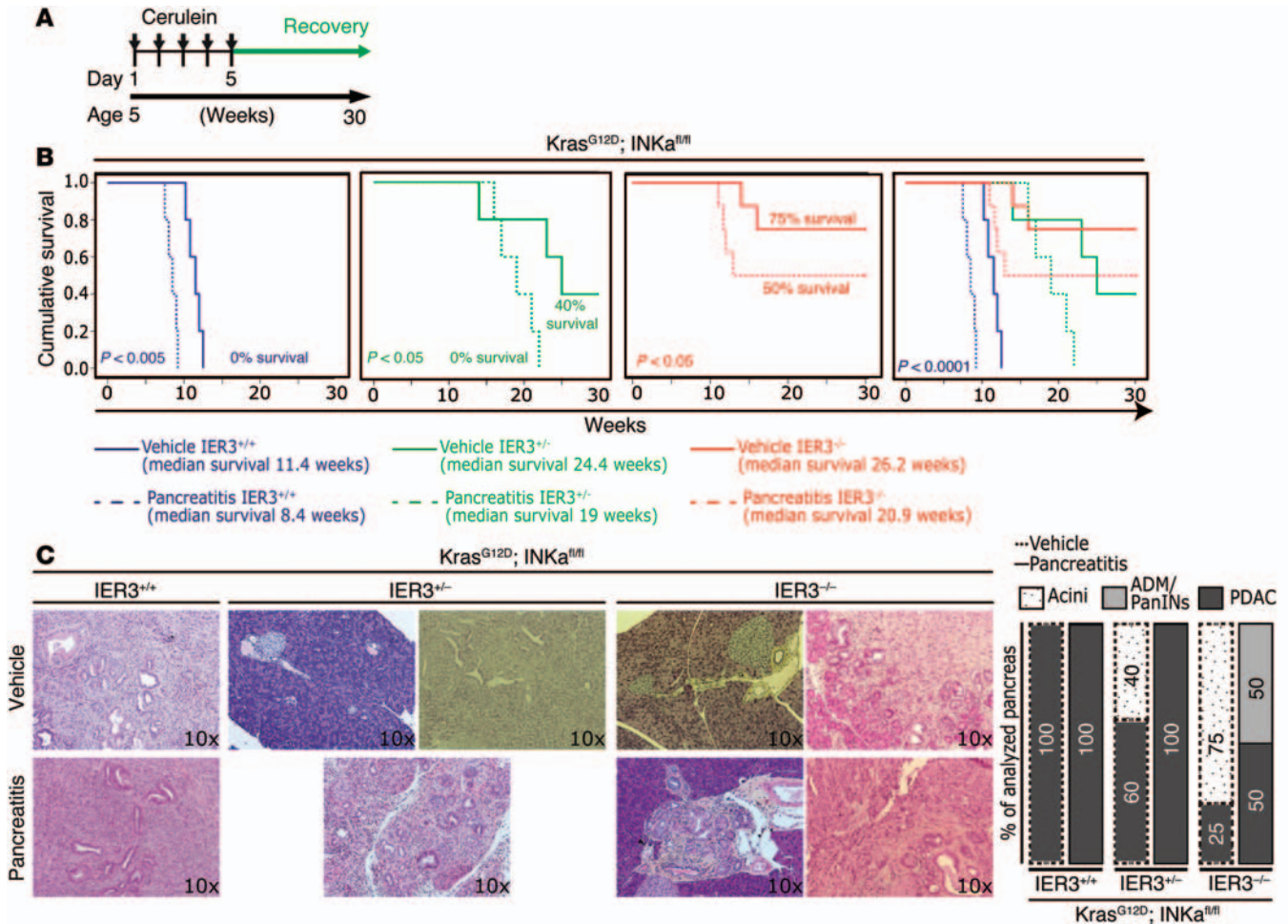
Figure 6. IER3 is necessary for pancreatitis-associated tumorigenesis in *Kras^G12D*;*Ink4a^fl/fl*;*Ier3*^+/+ mice. *Kras^G12D*;*Ink4a^fl/fl*;*Ier3*^+/+, *Kras^G12D*;*Ink4a^fl/fl*;*Ier3*^+/−, and *Kras^G12D*;*Ink4a^fl/fl*;*Ier3*^−/− mice were treated with cerulein or vehicle and then analyzed for progression to PDAC during recovery (**A**). (**B**) Kaplan-Meier analysis of cumulative survival, comparing cerulein-treated versus untreated animals for each genotype (*Kras^G12D*;*Ink4a^fl/fl*;*Ier3*^+/+, $P < 0.005$, $n = 5$; *Kras^G12D*;*Ink4a^fl/fl*;*Ier3*^+/−, $P < 0.05$, $n = 5$; *Kras^G12D*;*Ink4a^fl/fl*;*Ier3*^−/−, $P > 0.05$, $n = 8$) and among all genotypes ($P < 0.0001$). (**C**) H&E staining of mice treated with saline vehicle or cerulein, and quantified proportions of lesion types in tissue.

delayed both PanIN and PDAC development, these were accelerated by pancreatitis induction to a significantly lesser extent in the *Ier3*-deficient mice (Figures 5 and 6), which indicated that other pancreatitis-associated factors besides IER3 are involved in PanIN and PDAC development. One of these factors could be EGFR, since it is activated in pancreas with pancreatitis and its inactivation inhibits *Kras*-dependent PDAC development in mice (38, 46). Recently, Kawahara and colleagues found that IER3 protein was highly expressed in response to EGF stimulation along with enhanced p-ERK1/2 (47). This result suggests the possibility of cross-talk between the EGFR and IER3 pathways, since signals emanating from an active EGFR are transduced by p-ERK1/2. Thus, our present findings extend the knowledge of how MAPKs are regulated in order to transduce oncogenic signals from stimuli that activate *Kras*. Thus, combining observations in human tissue with cellular and molecular studies as well as in vivo genetic models for initiation (*Kras^G12D*) and progression (*Kras^G12D*;*Ink4a^fl/fl* and cerulein-treated *Kras^G12D*) may shed light on the types of pathways that further regulate these processes.

Importantly, we observed positive immunostaining for p-MEK1/2 in nontransformed areas within the pancreas of *Kras^G12D* mice, which was expected since MEK1/2 is a downstream factor of oncogenic *Kras*. However, p-ERK1/2 immunostaining appeared negative in acini pancreatic cells, which indicates that although oncogenic *Kras* signaling efficiently activates MEK1/2, a downstream regulator of p-ERK1/2 is dampening this signal could therefore inhibit the oncogenic *Kras* effect. According to our findings, the phosphatase PP2A seems to be one of these factors. Interestingly, immunostaining of p-ERK1/2 and IER3 was positive in ADM and PanINs. We therefore hypothesize that factors inhibiting PP2A phosphatase activity (such as IER3) could facilitate the *Kras* oncogenic effects, leading to transformation, whereas in areas in which PP2A activity remains conserved, *Kras*-driven transformation does not occur. Indeed, IER3 expression was observed in early transformation processes such as ADM and early PanINs, but decreased or even disappeared in late PanINs and PDAC, especially in poorly differentiated tumors (Figure 1, B and C), which supports the idea that IER3 is necessary for the

initial (tumor initiation) rather than latter steps during pancreatic carcinogenesis. It is important to note that IER3 was overexpressed in peritumoral pancreatic tissue, an area in which ADM and PanINs are frequently found. Thus, we speculate that IER3 expression is involved in the development of these lesions. In support of this idea, we showed that modifications of IER3 activity in PDAC-derived cells, and its consequences on p-ERK1/2, had almost no effect on tumor growth when xenografted in nude mice (Supplemental Figure 3). These data are in agreement with clinical observations that ERK1/2 inhibitors are an inefficient treatment for patients with PDAC.

Our results must be discussed in comparison with a previous study by Sasada and colleagues, who studied 78 patients with PDAC and found that 53% had positive staining for IER3 in the pancreas, which correlated with a better survival time than patients with negatively stained tumors (33). In contrast, we recently reported that expression of IER3 was associated with a poor prognosis in a group of 34 patients with PDAC (6). We currently cannot explain this difference, although the discrepancy likely results from IER3 detection in different stages and different types of PDAC. Nevertheless, in the present work, we unambiguously found that IER3 was upregulated in ADM and low-grade PanINs, at levels that were higher in well-to-moderately differentiated than in poorly differentiated tumors (Figure 1, A–D). Thus, we conclude that although IER3 is an important regulator of PDAC development, it does not function as a reliable prognostic marker for PDAC patients since its expression changes during disease progression, with higher levels at the early phases and lower levels at the late ones. In contrast, from our previous studies and the work reported herein, we infer that an important functional role for IER3 in PanIN formation and PDAC development is mediated through its effect on PP2A activity, which affects p-ERK1/2 stability. However, since IER3 is a multifunctional factor, additional work is required to define whether this protein exerts additional protumoral effects through interference with other signaling pathways, in particular NF-κB (10, 48) and PI3K/AKT (17). Similarly, with respect to cellular mechanisms, it is possible that this protein additionally modulates pancreatic carcinogenesis by modifying immunological responses (49, 50) and apoptosis (10, 11, 28, 51), which are well-characterized players in the process of pancreatic cell transformation. Thus, our present findings not only extend the existing knowledge in the field, but also generate the rational for additional studies.

In conclusion, we have shown that IER3 plays an important role in supporting the oncogenic effect of $Kras^{G12D}$ in pancreas by sustaining p-ERK1/2, probably by inhibiting the phosphatase PP2A. Given that $Kras$ is mutated in the majority of pancreatic cancer, the mechanisms by which its oncogenic signals are modulated by distinct effectors, such as IER3, bear significant biomedical relevance.

Methods

Mice. $Kras^{G12D}$ ($Pdx1$-$Cre;LSL$-$Kras^{G12D}$), $Kras^{G12D};Ink4a^{fl/fl}$ ($Pdx1$-$cre;LSL$-$Kras^{G12D};Ink4a^{fl/fl}$), and $Ier3^{-/-}$ strains have been described elsewhere (6, 35, 37). Pancreatitis was induced by cerulein (Sigma-Aldrich) administration i.p. at 250 μg/kg body weight; we used

2 models of recurrent pancreatitis followed by a recovery time (Figure 5, D and E, and Figure 6A). Because animals were from different genetic backgrounds, we systematically used littermate control and experimental mice. Moreover, in each obtained pancreas sampled, LSL-$Kras^{G12D}$ recombination was checked by PCR, as previously described (3).

Cell culture and transfections. MiaPaCa2 and Panc1 cells obtained from ATCC were maintained in DMEM (Invitrogen) supplemented with 10% FBS at 37°C with 5% CO_2. INTERFERin reagent (Polyplus-transfection) was used to perform siRNA transfections according to the manufacturer's protocol. Scrambled siRNA, targeting no known gene sequence, was used as negative control. The sequences of IER3-specific siRNA were previously reported (6). Active ERK1/2 analysis by flow cytometry was performed by standard staining protocol on a FACSCalibur flow cytometer (BD Biosciences). Data analysis was performed using CellQuest (BD Biosciences) or FlowJO (Treestar) software. Lipofectamine 2000 Transfection Reagent (Life Technologies) was used to perform plasmid transfections according to the manufacturer's protocol, and plasmids used were described previously (15, 16).

IHC and IF. Pancreatic sections were fixed in 4% paraformaldehyde and paraffin embedded. H&E and PAS IHC and IF were performed using standard procedures. Sections were probed with the following primary antibodies: p-ERK1/2 (phosphorylated p44/42 MAPK) (Thr202/Tyr204) (Cell Signaling) for IHC, p-ERK1/2 (Thr202/Tyr204) XP (Cell signaling) for IF and flow cytometry, p-MEK1/2 (Ser221) (Cell signaling) for IHC, pancreatic amylase antibody (Abcam), CK19 (Santa Cruz Biotechnology), and previously described anti-IER3 antiserum (15). Alexa Fluor 488 and 594 (Invitrogen) were used as secondary antibodies. Samples were mounted in ProLong Antifade Reagent with DAPI (Invitrogen) and examined using an Eclipse 90i Nikon microscope.

Quantification of IER3-positive lesions per tissue. The number of peritumoral acini and low- and high-grade PanINs were calculated by determining the number of IER3-positive lesions (as determined by IF or IHC) per tissue; data are expressed as the percentage of the total number of lesions in the tissue.

Quantification of lesions per mouse. The number of lesions per field was counted, and the lesion types were classified on H&E-stained slides. Values were quantified as the average of 15–20 ×20 fields of view from at least 5 mice per genotype.

Real-time quantitative PCR. Pancreas RNAs from human PDACs were prepared following Chirwin's protocol (52). RNA from cells was prepared using TRIZOL Reagent (Invitrogen) and reversed transcribed using Go Script (Promega) according to the manufacturer's instructions. Real-time quantitative PCR was performed in a Stratagene cycler using Takara reagents. The sequences of the primers used to amplify human *IER3* mRNA were 5′-CAGTCGAGGAACCGAACCC-3′ (forward) and 5′-GATCTGGCAGAAGACGATGGT-3′ (reverse).

Immunoblotting. Protein extraction was performed on ice using total protein extraction buffer (50 mM HEPES, pH 7.5; 150 mM NaCl; 20% SDS; 1 mM EDTA; 1 mM EGTA; 10% glycerol; 1% Triton; 25 mM NaF; 10 μM $ZnCl_2$; and 50 mM DTT). Before lysis, protease inhibitor cocktail at 1:200 (Sigma-Aldrich, NUPR1340), 500 μM PMSF, 1 mM sodium orthovanadate, and 1 mM β glycerophosphate were added. Protein concentration was measured using a BCA Protein Assay Kit (Pierce Biotechnology). Protein samples (60 μg) were denatured at

95°C and subsequently separated by SDS-PAGE. After transfer to nitrocellulose, membrane was blocking with 1% BSA, and samples were probed with primary antibody followed by horseradish peroxidase–coupled secondary antibody. Image acquisition was made using a Fusion FX image acquisition system (Vilber Lourmat), and bands were quantified with ImageJ (NIH).

3D acinar cell culture. Primary cultures of acini from *LSL-Kras^{G12D};Ier3$^{+/+}$* or *LSL-Kras^{G12D};Ier3$^{-/-}$* animals was performed as previously described (49). Briefly, mouse pancreas was immediately removed after euthanasia, cut into small pieces, and digested with 200 μg/ml collagenase P (Sigma-Aldrich) for 20 minutes at 37°C. Acini were collected by centrifugation and resuspended in 3D culture base medium (RPMI 1640 medium supplemented with 10% FBS, 0.1 mg/ml soybean trypsin inhibitor, 1 μg/ml dexamethasone, and antibiotics). 24-well plates were coated with a collagen layer (250 μl/well; Sigma-Aldrich) for 1 hour. Cell suspensions were mixed 1:1 with collagen and plated (0.5 ml/well). The cell/collagen mix was allowed to solidify for 1 hour at 37°C before addition of 1 ml 3D culture media. After treatment, acini were fixed with 4% paraformaldehyde and included in paraffin. 4-μm paraffin sections were H&E stained, and the percentage of acini that converted to ductal cysts was calculated by counting individual clusters in all wells.

Isolation of PDECs. Cells from mouse pancreatic ducts were isolated as previously described (38, 39). Briefly, main pancreatic ducts were manually dissected from *LSL-Kras^{G12D};Ier3$^{+/+}$* or *LSL-Kras^{G12D};Ier3$^{-/-}$* animals and digested with 2 mg/ml collagenase Type XI (Sigma-Aldrich) for 12 minutes at 37°C. Fragments were then digested again with 2 U/ml dispase I (Sigma-Aldrich), followed by 6 successive 5-minute digestions with 0.1% Trypsin (Invitrogen). Isolated PDECs were resuspended in pancreatic medium (DMEM/F-12 media [Gibco] supplemented with 100 ng/ml EGF [BD Biosciences], 40 μg/ml dexamethasone [Sigma-Aldrich], 2.5 mg/ml bovine pituitary extract [Sigma-Aldrich], 50 μM triiodo-L-thyronine [Sigma-Aldrich], 100 μg/ml cholera toxin [Quadratech], insulin/transferrin/selenium [BD Biosciences], 1 μg/ml soybean trypsin inhibitor [Sigma-Aldrich], and 10% FBS [GE Healthcare]), plated onto gridded coverslips coated with 2–5 μg/cm² laminin I (Sigma-Aldrich), and incubated at 37°C and 5% CO_2. After PDEC isolation, cells were incubated undisturbed for 48 hours. On the third day, cells were cycled by 24 hours of starvation (DMEM/F-12 media supplemented with 100 μg/ml cholera toxin, 1 μg/ml soybean trypsin inhibitor, and 0.25% FBS). The next day, cultures were alternatively infected with Ad-Cre or Ad-null viruses (MOI 11). Cells were evaluated for incorporation of BrdU.

BrdU assay. After 24 hours of adenovirus infection, PDECs were incubated with 10 μM BrdU (Sigma-Aldrich) for 48 hours and fixed in 4% paraformaldehyde. Cells were then treated with 2N HCl for 30 minutes, washed several time with PBS, blocked, and permeabilized by 1 hour of incubation in PBS with 5% FBS and 0.25% Triton X-100. Immunodetection of BrdU incorporation was performed with a mouse monoclonal anti-BrdU antibody (Sigma-Aldrich) in PBS with 1% BSA (overnight). Goat anti-mouse Alexa Fluor 594 (Invitrogen) was used as a secondary antibody. Slides were mounted with VECTASHIELD mounting medium with DAPI (Vector Laboratories). BrdU incorporation was estimated by counting BrdU-positive cells and expressed as the percentage of total nuclei (stained with DAPI); data are mean ± SEM of 500 cells counted in duplicate.

Primary mouse Kras^{G12D};Ink4a$^{fl/fl}$ pancreatic cell preparation. Primary PDAC cells from 2 *Kras^{G12D};Ink4a$^{fl/fl}$* mice were prepared as previously described (53). Briefly, 50 mg pancreatic tumor was chopped into pieces and disrupted in a 1-mg/ml solution of collagenase V (Sigma-Aldrich) in DMEM/F-12 (Gibco) at 37°C, washed in HBSS (5 mmol/l glucose and 0.05 mmol/l $CaCl_2$), and then separated into single cells by supplemental incubation in 0.05% Trypsin-EDTA (Invitrogen) before gentle washing and cultured in serum-free defined medium (SFDM) (53). After 24 hours, the culture medium was replaced by fresh SFDM, and cells were allowed to grow and passed as needed. 2 cell lines were obtained from different mice (CKΔI-1 and CKΔI-2).

Xenografts. Primary CKΔI-1 and CKΔI-2 cells were transfected with plasmids encoding for HA-IER3, HA-IER3-ΔBD, HA-IER3-T18A, ERK2-L73P/S151D, IER3 shRNA, or empty vector, as previously reported (15, 16), together with pcDNA3.1/Puro to select transfected cells using Lipofectamine 2000 Transfection Reagent (Invitrogen). MiaPaCa2 and Panc1 cells were transfected with IER3 shRNA or scrambled shRNA vector together with pcDNA3.1/Puro using the same transfection agent. After 10 days of antibiotic selection, cells were implanted subcutaneously in male nude mice 4–6 weeks of age with a metal trocar. Tumor size was measured with an external caliper once weekly, and volume was calculated as $(4\pi/3) \times (w/2)^2 \times (l/2)$. Each experimental group consisted of at least 3 mice.

Statistics. To compare IER3-positive lesions per tissue, 1-way ANOVA was used to calculate significance among groups. To compare *IER3* mRNA expression among groups (well-to-moderately differentiated and poorly differentiated adenocarcinoma), 1-way ANOVA was used, and *P* values were calculated by $2^{-\Delta\Delta Ct}$ as described previously (54). To compare lesion number per field among *Kras^{G12D};Ier3$^{+/+}$*, *Kras^{G12D};Ier3$^{+/-}$*, and *Kras^{G12D};Ier3$^{-/-}$* mice at 14, 25, and 40 weeks of age, 2-way ANOVA was used. Survival was analyzed by Kaplan-Meier test. Values were expressed as mean ± SEM. All tests of significance were 2-tailed, and the level of significance was set at 0.05. All cell line data shown are representative of at least 4 independent experiments. All statistical test were performed using IBM SPSS statistics 21.

Study approval. Mice were kept within the Experimental Animal House of the Centre de Cancérologie de Marseille (CRCM), pole Luminy, following institutional guidelines.

Address correspondence to: Juan L. Iovanna, INSERM U1068, CRCM, Stress Cell, UNK 13288 Marseille Cedex 9, France. Phone: 33.491.828803; E-mail: juan.iovanna@inserm.fr.

1. Maitra A, Hruban RH. Pancreatic cancer. *Annu Rev Pathol*. 2008;3:157–188.

2. Almoguera C, Shibata D, Forrester K, Martin J, Arnheim N, Perucho M. Most human carcinomas of the exocrine pancreas contain mutant c-K-ras genes. *Cell*. 1988;53(4):549–554.

3. Hingorani SR, et al. Preinvasive and invasive ductal pancreatic cancer and its early detection in the mouse. *Cancer Cell*. 2003;4(6):437–450.

4. Kanda M, et al. Presence of somatic mutations in most early-stage pancreatic intraepithelial neoplasia. *Gastroenterology*. 2012;142(4):730–733.

5. Hong SM, Park JY, Hruban RH, Goggins M. Molecular signatures of pancreatic cancer. *Arch Pathol Lab Med*. 2011;135(6):716–727.

6. Hamidi T, et al. Nuclear protein 1 promotes pancreatic cancer development and protects cells from stress by inhibiting apoptosis. *J Clin Invest*. 2012;122(6):2092–2103.

7. Wu MX. Roles of the stress-induced gene IEX-1 in regulation of cell death and oncogenesis. *Apoptosis*. 2003;8(1):11–18.

8. Arlt A, Schafer H. Role of the immediate early response 3 (IER3) gene in cellular stress response, inflammation and tumorigenesis. *Eur J Cell Biol*. 2011;90(6):545–552.

9. Gonzalez S, Perez-Perez MM, Hernando E, Serrano M, Cordon-Cardo C. p73β-Mediated apoptosis requires p57kip2 induction and IEX-1 inhibition. *Cancer Res*. 2005;65(6):2186–2192.

10. Wu MX, Ao Z, Prasad KV, Wu R, Schlossman SF. IEX-1L, an apoptosis inhibitor involved in NF-κB-mediated cell survival. *Science*. 1998;281(5379):998–1001.

11. Yoon S, et al. IEX-1-induced cell death requires BIM and is modulated by MCL-1. *Biochem Biophys Res Commun*. 2009;382(2):400–404.

12. Pearson G, et al. Mitogen-activated protein (MAP) kinase pathways: regulation and physiological functions. *Endocr Rev*. 2001;22(2):153–183.

13. Marshall CJ. Specificity of receptor tyrosine kinase signaling: transient versus sustained extracellular signal-regulated kinase activation. *Cell*. 1995;80(2):179–185.

14. Murphy LO, Smith S, Chen RH, Fingar DC, Blenis J. Molecular interpretation of ERK signal duration by immediate early gene products. *Nat Cell Biol*. 2002;4(8):556–564.

15. Garcia J, Ye Y, Arranz V, Letourneux C, Pezeron G, Porteu F. IEX-1: a new ERK substrate involved in both ERK survival activity and ERK activation. *EMBO J*. 2002;21(19):5151–5163.

16. Letourneux C, Rocher G, Porteu F. B56-containing PP2A dephosphorylate ERK and their activity is controlled by the early gene IEX-1 and ERK. *EMBO J*. 2006;25(4):727–738.

17. Rocher G, Letourneux C, Lenormand P, Porteu F. Inhibition of B56-containing protein phosphatase 2As by the early response gene IEX-1 leads to control of Akt activity. *J Biol Chem*. 2007;282(8):5468–5477.

18. Han L, Geng L, Liu X, Shi H, He W, Wu MX. Clinical significance of IEX-1 expression in ovarian carcinoma. *Ultrastruct Pathol*. 2011;35(6):260–266.

19. Lee YH, Kim JH, Zhou H, Kim BW, Wong DT. Salivary transcriptomic biomarkers for detection of ovarian cancer: for serous papillary adenocarcinoma. *J Mol Med (Berl)*. 2012;90(4):427–434.

20. Prall WC, et al. Differential gene expression of bone marrow-derived CD34+ cells is associated with survival of patients suffering from myelodysplastic syndrome. *Int J Hematol*. 2009;89(2):173–187.

21. Haase D, et al. New insights into the prognostic impact of the karyotype in MDS and correlation with subtypes: evidence from a core dataset of 2124 patients. *Blood*. 2007;110(13):4385–4395.

22. Hofmann WK, de Vos S, Komor M, Hoelzer D, Wachsman W, Koeffler HP. Characterization of gene expression of CD34+ cells from normal and myelodysplastic bone marrow. *Blood*. 2002;100(10):3553–3560.

23. Steensma DP, et al. Rearrangements and amplification of IER3 (IEX-1) represent a novel and recurrent molecular abnormality in myelodysplastic syndromes. *Cancer Res*. 2009;69(19):7518–7523.

24. Davids MS, Steensma DP. The molecular pathogenesis of myelodysplastic syndromes. *Cancer Biol Ther*. 2010;10(4):309–319.

25. Ria R, et al. Gene expression profiling of bone marrow endothelial cells in patients with multiple myeloma. *Clin Cancer Res*. 2009;15(17):5369–5378.

26. Wu J, Nihal M, Siddiqui J, Vonderheid EC, Wood GS. Low FAS/CD95 expression by CTCL correlates with reduced sensitivity to apoptosis that can be restored by FAS upregulation. *J Invest Dermatol*. 2009;129(5):1165–1173.

27. Zhang Y, Finegold MJ, Porteu F, Kanteti P, Wu MX. Development of T-cell lymphomas in Emu-IEX-1 mice. *Oncogene*. 2003;22(44):6845–6851.

28. Akilov OE, Wu MX, Ustyugova IV, Falo LD, Falo LD Jr, Geskin LJ. Resistance of Sezary cells to TNF-α-induced apoptosis is mediated in part by a loss of TNFR1 and a high level of the IER3 expression. *Exp Dermatol*. 2012;21(4):287–292.

29. Yang C, et al. Identification of cyclin D1- and estrogen-regulated genes contributing to breast carcinogenesis and progression. *Cancer Res*. 2006;66(24):11649–11658.

30. Nambiar PR, et al. Genetic signatures of high- and low-risk aberrant crypt foci in a mouse model of sporadic colon cancer. *Cancer Res*. 2004;64(18):6394–6401.

31. Ustyugova IV, Zhi L, Abramowitz J, Birnbaumer L, Wu MX. IEX-1 deficiency protects against colonic cancer. *Mol Cancer Res*. 2012;10(6):760–767.

32. Segditsas S, et al. Putative direct and indirect Wnt targets identified through consistent gene expression changes in APC-mutant intestinal adenomas from humans and mice. *Hum Mol Genet*. 2008;17(24):3864–3875.

33. Sasada T, et al. Prognostic significance of the immediate early response gene X-1 (IEX-1) expression in pancreatic cancer. *Ann Surg Oncol*. 2008;15(2):609–617.

34. Wu MX, Ustyugova IV, Han L, Akilov OE. Immediate early response gene X-1, a potential prognostic biomarker in cancers. *Expert Opin Ther Targets*. 2013;17(5):593–606.

35. Cano CE, et al. Genetic inactivation of Nupr1 acts as a dominant suppressor event in a two-hit model of pancreatic carcinogenesis. *Gut*. 2014;63(6):984–995.

36. Tuveson DA, et al. Mist1-KrasG12D knock-in mice develop mixed differentiation metastatic exocrine pancreatic carcinoma and hepatocellular carcinoma. *Cancer Res*. 2006;66(1):242–247.

37. Sommer SL, et al. Elevated blood pressure and cardiac hypertrophy after ablation of the gly96/IEX-1 gene. *J Appl Physiol*. 2006;100(2):707–716.

38. Agbunag C, Bar-Sagi D. Oncogenic K-ras drives cell cycle progression and phenotypic conversion of primary pancreatic duct epithelial cells. *Cancer Res*. 2004;64(16):5659–5663.

39. Agbunag C, Lee KE, Buontempo S, Bar-Sagi D. Pancreatic duct epithelial cell isolation and cultivation in two-dimensional and three-dimensional culture systems. *Methods Enzymol*. 2006;407:703–710.

40. Ji B, et al. Ras activity levels control the development of pancreatic diseases. *Gastroenterology*. 2009;137(3):1072–1082.

41. Gidekel Friedlander SY, et al. Context-dependent transformation of adult pancreatic cells by oncogenic K-Ras. *Cancer Cell*. 2009;16(5):379–389.

42. Guerra C, et al. Chronic pancreatitis is essential for induction of pancreatic ductal adenocarcinoma by K-Ras oncogenes in adult mice. *Cancer Cell*. 2007;11(3):291–302.

43. Alessi DR, Gomez N, Moorhead G, Lewis T, Keyse SM, Cohen P. Inactivation of p42 MAP kinase by protein phosphatase 2A and a protein tyrosine phosphatase, but not CL100, in various cell lines. *Curr Biol*. 1995;5(3):283–295.

44. Janssens V, Goris J. Protein phosphatase 2A: a highly regulated family of serine/threonine phosphatases implicated in cell growth and signalling. *Biochem J*. 2001;353:417–439.

45. McCright B, Rivers AM, Audlin S, Virshup DM. The B56 family of protein phosphatase 2A (PP2A) regulatory subunits encodes differentiation-induced phosphoproteins that target PP2A to both nucleus and cytoplasm. *J Biol Chem*. 1996;271(36):22081–22089.

46. Lee JT, et al. Colonic histoplasmosis presenting as colon cancer in the nonimmunocompromised patient: report of a case and review of the literature. *Am Surg*. 2004;70(11):959–963.

47. Kawahara E, Maenaka S, Shimada E, Nishimura Y, Sakurai H. Dynamic regulation of extracellular signal-regulated kinase (ERK) by protein phosphatase 2A regulatory subunit B56γ1 in nuclei induces cell migration. *PLoS One*. 2013;8(5):e63729.

48. Arlt A, et al. The early response gene IEX-1 attenuates NF-κB activation in 293 cells, a possible counter-regulatory process leading to enhanced cell death. *Oncogene*. 2003;22(21):3343–3351.

49. Shi G, DiRenzo D, Qu C, Barney D, Miley D, Konieczny SF. Maintenance of acinar cell organization is critical to preventing Kras-induced acinar-ductal metaplasia. *Oncogene*. 2013;32(15):1950–1958.

50. Sasada T, et al. Immediate early response gene X-1, a stress-inducible antiapoptotic gene, encodes cytotoxic T-lymphocyte (CTL) epitopes capable of inducing human leukocyte antigen-A33-restricted and tumor-reactive CTLs in gastric cancer patients. *Cancer Res*. 2004;64(8):2882–2888.

51. Ishimoto Y, Satsu H, Totsuka M, Shimizu M.

IEX-1 suppresses apoptotic damage in human intestinal epithelial Caco-2 cells induced by co-culturing with macrophage-like THP-1 cells. *Biosci Rep*. 2011;31(5):345–351.

52. Chirgwin JM, Przybyla AE, MacDonald RJ, Rut-ter WJ. Isolation of biologically active ribonucle-ic acid from sources enriched in ribonuclease. *Biochemistry*. 1979;18(24):5294–5299.

53. Schreiber FS, et al. Successful growth and charac-terization of mouse pancreatic ductal cells: func-tional properties of the Ki-RAS(G12V) oncogene. *Gastroenterology*. 2004;127(1):250–260.

54. Yuan JS, Reed A, Chen F, Stewart CN, Stewart CN Jr. Statistical analysis of real-time PCR data. *BMC Bioinformatics*. 2006;7:85.